SOLDERING CHARACTERISTICS AND THERMO-MECHANICAL PROPERTIES OF Pb-FREE SOLDER PASTE FOR REFLOW SOLDERING

A.M. Najib[1], M.Z. Abdullah[2], A.A. Saad[2], F. Che Ani[3] and Z. Samsudin[3]

[1]Faculti Kejuruteraan Pembuatan,
Universiti Teknikal Malaysia Melaka, Hang Tuah Jaya, 76100 Durian Tunggal, Melaka, Malaysia.

[2]School of Mechanical Engineering,
Universiti Sains Malaysia, Engineering Campus,14300,
Nibong Tebal, Penang, Malaysia.

[3]Jabil Circuit Sdn. Bhd.,
Bayan Lepas Industrial Park, 11900, Penang, Malaysia.

Corresponding Author's Email: [1]najibali@utem.edu.my

Article History: Received 7 December 2018; Revised 10 April 2019; Accepted 9 August 2019

ABSTRACT: A deep understanding in thermal characteristics of lead-free solder paste grades is one of the most crucial factors when dealing with reflow soldering process. These temperatures are critical parameters for proper settings of the real reflow process. This report is devoted to discussing the findings obtained during utilization of differential scanning calorimetry (DSC) and calculation using MATLAB to identify the latent heat, solidus and liquidus temperature, and surface tension applicable to numerically simulate the real process of reflow soldering. It can be stated that the equilibrium solidus and liquidus temperatures during solidification process are not a reversal of the melting process, with the solid phase equilibrium occurred at a lower temperature due to the difficulty of ß-Sn nucleation. Amount of heat energy released during solidification differs less than 10% for SAC405 and less than 1% for SAC105 with the latent heat of fusion during the melting process.

KEYWORDS: *DSC; SAC Solder; Reflow Soldering; Temperature Profile*

1.0 INTRODUCTION

The enforcement to abandon Pb in electronics was imposed by the European Union started on July 2006 [1]. As a consequence, intensive search for alternative replacement of lead was become the primary concern in electronics industry. Eventually, the SAC solder offering

the most reliable solution for this issue, as having the closest melting point with the conventional solder. The eutectic composition of 63Sn-37Pb has a eutectic liquidus temperature of 183°C whereas the eutectic composition of SAC solder melting temperature is 217°C. Pure Tin (Sn) has a melting temperature of 232°C. There is temperature reduction of 49°C with the addition of Pb element in Sn at eutectic composition. In case of the eutectic composition of SAC solder, there is temperature reduction of 15°C with the addition of combined Ag element and Cu element in Sn. In this study, the thermo-mechanical data for the lead-free solder will be identified using dynamic thermal analysis method.

The differential scanning calorimetry (DSC) is a thermal analysis instrumentation based on the caloric value of heat fusion. The principle is based on direct measurement of the temperature of a sample, subjected to continuous changes of heating and cooling. The result is presented as a heating and cooling curve. It is possible to obtain temperature related parameters such as latent heat, liquidus and solidus temperature.

The basic principle of the method is a measurement of the temperature difference (heat-flow difference) between the measured sample and the reference. The reference is usually an empty pan placed on reference location. The sample and reference are subjected to the same setting of the temperature program of the continuous heating rate and cooling rate. The result is a DSC curve expressing the dependence of the temperature gradient between the measured sample and the reference. Any ongoing phase transformation in the sample, deflection from baseline is formed. It is possible to obtain the temperatures of phase transformations by interpreting the deflection points for given experimental conditions.

Apart from the dynamic method of thermal analysis, it is possible to obtain the temperature of the solidus and liquidus temperature of solder using calculation method using software package such as Pandat or Computherm. Different kinds of thermodynamic properties can be calculated using embedded equations in the software.

There was various lead-free solder developed by various researchers and it was recommended by various organizations. National Electronics Manufacturing Initiative (NEMI) research group originate from the USA recommended Sn-Ag-Cu (SAC) solder specifically SAC396 [1]. Active research focusing on SAC solder has been conducted to narrowed down the knowledge gap of the recommended lead free solder especially SAC solder [2-5]. An EU consortium project (IDEALS) have recommended near eutectic alloy Sn-3.8Ag-0.7Cu(SAC387)

[1]. The SAC solder implementation were inline with the proposed technology roadmap for electronic packaging industry presented by International Electronics Manufacturing Initiative (iNEMI) research group [6-7]. Japan Electronics and Information Technology Industries (JEITA) recommended Sn-2.5 Ag-(0.5-1.0) Cu and Sn-3.0 Ag-0.5 Cu alloy (SAC 305). Recent development also promotes new implementation of nanoparticles reinforcement in solder joint [8]. Composition of reinforcing elements such as NiO [9], Al_2O_3 [10], and pure element of Ni, Bi, and Fe [11-12] in SAC alloys reported to enhance the mechanical properties and the service reliability of SAC solder.

To the author knowledge, there are still no exact alloy replacements of 63Sn-37Pb that is suitable for all applications and possess similar or better reliability. However, several SAC solder alloys with different compositions are either recommended by different associations or used as solder alloy in practice. Up to now, Sn-Ag-Cu alloys are still favoured practically as lead-free solutions for interconnections in the microelectronic packaging sector, in the form of solder balls and solder pastes. It is apparent that further study of SAC solder is needed to fill in current knowledge gap regarding various SAC solder. Compare to the lead solder (63Sn-37Pb), most knowledge is already adequate and completed. This report details the attempt to determine the mechanical data of SAC solder alloy with various silver content. Experimental analysis using the differential scanning calorimetry (DSC) has been conducted with the objective, to study the thermo-mechanical data of selected SAC solder and compare the results with the conventional Sn-37Pb solder. Results will be discussed in terms of the specific heat capacity, density and surface tension values.

2.0 EXPERIMENTAL

Specific heat capacity, solidus temperature, liquidus temperature and latent heat will be determined experimentally using differential scanning calorimetry (DSC) equipment. The temperature range of measurement is 40°C to 280°C. The alloy density and surface tension will be calculated using MATLAB. Some of the resulted values will be compared with the data from the literature review.

Determination of selected thermal parameters during heating and cooling of solder paste was realized with the dynamic method of thermal analysis. Differential Scanning Calorimetry from National Instruments, TA DSC Q20 model located in the Nanofabrication Laboratory (USM) was used for the experiments, as depicted in Figure 1. The liquidus

temperature, solidus temperature, and latent heat were determined for the numerical simulation of actual reflow soldering process.

Figure 1: DSC Equipment of TA DSC Q20

Commercially available solder paste specimens with various percentage of silver content namely SAC 105 (1%), SAC 305 (3%) and SAC 405 (4%), have been tested in this current study. It is essential to ensure uniform spreading of solder paste against the bottom of the pan for improved thermal contact. Therefore, the paste was spread carefully inside the Tzero pan. Then, the aluminium hermetic lid was used to sealed and encapsulated the pan with pressure applied by the Tzero Press. A weight limitation of DSC samples in the range of 5 to 15 miligrams was imposed to minimize the impact of the higher mass. The Pure Argon gas was set at 50 mL/min through out the experiment. In the cooling stage, liquid nitrogen coolant was manually introduced into a quench container, which was connected to the sample chamber. The quench container filled with liquid nitrogen will become the main source of cooling medium during the experiment. The instruments will control the cooling rate based on the prior setting in the experiment. The measured temperature was restricted from 40°C to 280°C. The ramp heating and ramp cooling rate were set at 20°C/min. Table 1 shows the characteristic features of the experiment.

Table 1: Experimental parameters of Differential Scanning Calorimetry (DSC)

Parameter	**TA DSC Q20**
Temperature Range	40°C – 280°C
Heating rate	20°C/min
Cooling rate	20°C/min
Temperature programm	Equilibrate,Ramp heating, Isothermal, Ramp cooling
Sample mass	5-15 mg
Atmosphere	Argon (50 mL/min)
Pan type	Tzero Pan with Tzero Hermetic Lid

The measurements carried out in the laboratory are focused on determining the thermo-physical properties such as an equilibrium temperature, the phase-change temperatures and the latent heat. In the DSC experiment, the temperature value near to equilibrium is quantitatively designed to approximate the equilibrium state.

The heat capacity of the solder paste was measured in several series of DSC test. In an ideal DSC experiment, a preliminary run on empty aluminium tzero pan was conducted to determineand the baseline value. Then, the DSC experiment using sapphire crimp pan was carried out to provide the opportunity for good sample-atmosphere interaction. Finally, the encapsulated solder paste samples in the aluminium pan were run for analysis. Similar experimental setting was adapted in all run condition.The result of heat flow curves of all run was illustrated in Figure 2. From the curves, the calometric value of specific heat capacity, C_p was calculated.

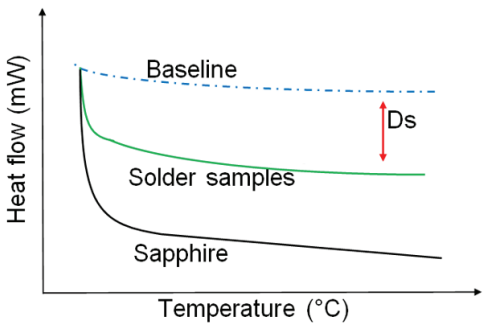

Figure 2: The heat flow curves of the specific heat capacity calculation

The specific heat capacity, C_p was calculated as follows:

$$C_p = \frac{60.D_s}{H_r.W_s}.E \quad (1)$$

where W_s represents the sample mass, D_s is the heat flow gradient, H_r is the rate of heating process, and E is the ratio of the standard sapphire heat capacity and the real sapphire heat capacity during the experiment. The experiment was repeated to get the average value of the specific heat capacity.

Besides, the surface tension in accordance to the Butler's model is calculated, as published in [13]. Based on the Butler model, the

equilibrium between a bulk phase and the surface layer of each element was taking into account. Hence, the surface tension value can be estimated using Equation (2):

$$\sigma_{\mathrm{SnAgCu}} = \sigma_{AgCu}\frac{Z_{\mathrm{Cu}}}{Z_{\mathrm{Cu}}+Z_{\mathrm{Sn}}} + \sigma_{AgSn}\frac{Z_{Cu}}{Z_{Cu}+Z_{Sn}} + \Delta\sigma_{\mathrm{CuSn}}(1-Z_{Ag}-Z_{Cu}) + \Delta\sigma_{SnAgCu} \quad (2)$$

The density of the solder alloy is calculated using following terms:

$$\rho_{\mathrm{SnAgCu}} = 1/\left(\frac{Z_{Sn}}{\rho_{Sn}} + \frac{Z_{Ag}}{\rho_{Ag}} + \frac{Z_{Cu}}{\rho_{Cu}}\right) \quad (3)$$

where ρ is the solder density and Z_{Sn},Z_{Ag},Z_{Cu} are the mass fraction of the metal element. This calculation only valid with the assumption of that minimal interaction or zero interaction between the mixture. Any changes in density due to temperature rises and intermetallics bonding was also neglected.

3.0 RESULTS AND DISCUSSION

Figure 3 indicates the specific heat capacities of the solder specimens over the measured temperature range. From the Figure 3, a slight increase of the specific heat capacity can be observed up to 105°C. The value then gradually decrease until the temperature reach 150°C.

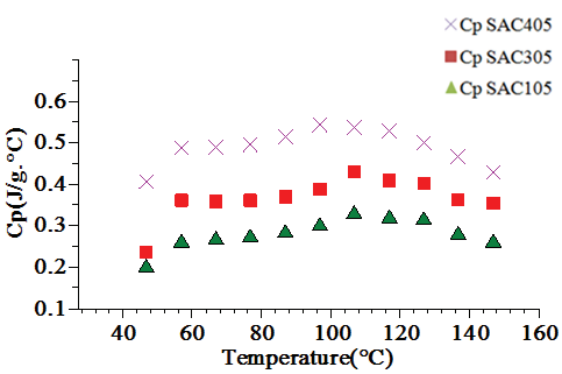

Figure 3: Experimental values for the specific heat capacity

As expected from the result, the SAC 405 with 4% silver content have the highest value of heat capacity amongst others. It is attributed from the fact, that the heat capacity of the pure silver was higher compared to the heat capacity of pure tin. The slight decrease in heat capacity was observed starting at 105°C possibly due to the interaction between flux and the solder particles. Table 2 indicates the results of the thermo-physical properties calculated from the DSC experiment, with the consideration of that the equilibrium state is achieved approximately equal at the temperature being almost equilibrium.

Table 2: Thermo-physical data for various solder

Solder Type	Average Cp (J/(g.°C)	Melting Latent Heat (J/g)	Solidification Latent Heat (J/g)
SAC405	0.491	55	49.82
SAC305	0.366	53.08	50.32
SAC105	0.279	52.33	51.92

Figure 4 shows the heat flow of SAC 105 solder paste sample in the function of peak temperature. From the Figure 4, it is evident that the SAC 105 solder shows an onset melting temperature of 218.47°C during heating process. This onset temperature corresponds to the ternary eutectic reaction of SAC alloy. Two peaks were observed at 221.19°C and 228.69°C in SAC 105 indicating the eutectic temperature for Sn-Ag (Ag_3 Sn + Sn) and Sn-Cu (Cu_6 Sn_5), respectively [14]. The SAC 105 reached the melting point at 238.12°C, wheares the onset solidification temperature was 206.86°C, where the nucleation temperature was determine by the onset solidification of the exothermic peak.

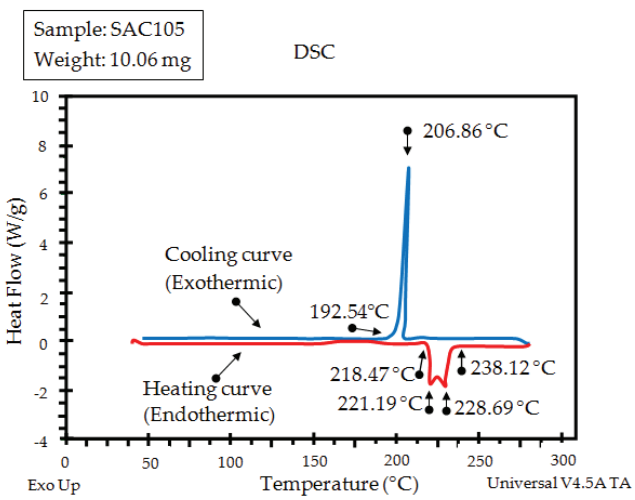

Figure 4: The heat flow of SAC 105 solder paste as a function of peak temperature

In the case of the SAC 305 solder paste sample, a clear evidence of onset melting point and solidification phase was clearly observed, as indicated in Figure 5. During the heating process, the SAC 305 exhibited an onset melting temperature of 218.02°C, which corresponds to the ternary eutectic activity of SAC alloy. An endothermic peak was detected during melting at 223.39°C in SAC 305, whereas the onset solidification of the exothermic peak during solidifation phase occurs at 200.67°C.

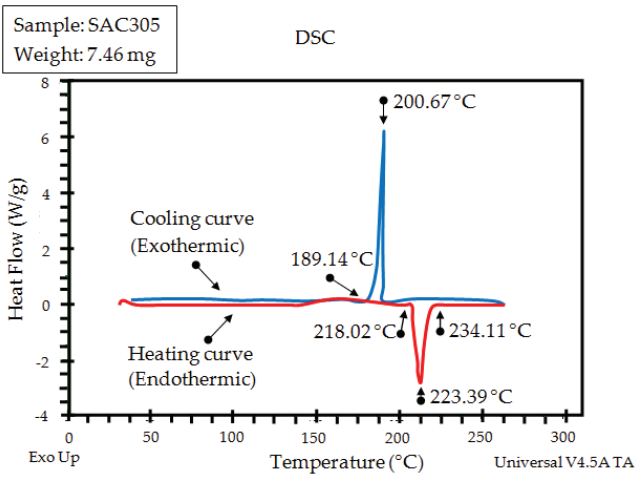

Figure 5: The heat flow of SAC 305 solder paste as a function of peak temperature

An identical trend was also obtained for the SAC 405 solder paste sample, as shown in Figure 6. The onset melting point of SAC 405 solder is achieved at 219.21°C. An endothermic peak during DSC heating was observed at 221.64°C in SAC 405. The SAC405 is fully melted at 232.01°C. During cooling, the nucleation temperature of the SAC 405 is at 199.09°C.

The cooling curve for all of the selected solder alloys shows the existence of metastable phase formation. The behavior is dominant as the amount of Sn in the solder alloy is dominant. The stable liquid phase after melting process does not nucleate easily during the cooling process.

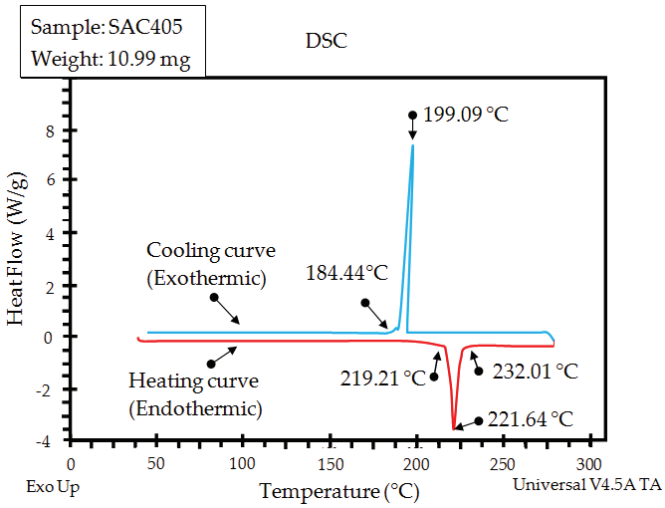

Figure 6: The heat flow of SAC 405 solder paste as a function of peak temperature

Figure 7 depicted the plot of surface tension of the ternary alloys at various temperature based on the Butler's model calculation. From the figure, a clear trend can be seen, in which the surface tension of all SAC solder alloy decreases almost linearly with the rise of temperature. The significant reduction in the surface tension values of the solder alloys is mainly attributed from the decreasing of the cohesive force as the molecular thermal activity increases internally. Table 3 presents the obtained density and average value of the surface tension for the solder alloy. The resulted densities of the SAC alloys from the calculation were 7.316g/cm³ for SAC 105, 7.361g/cm³ for SAC 305 and 7.384g/cm³ for SAC 405. A reference density value selected for the calculation is 10.49g/cm³ for Silver (Ag), 8.92g/cm³ for Copper (Cu), and 7.29g/cm³ for Tin (Sn). Noted that the surface tension and density calculation were obtained from Equations (2) and (3), respectively.

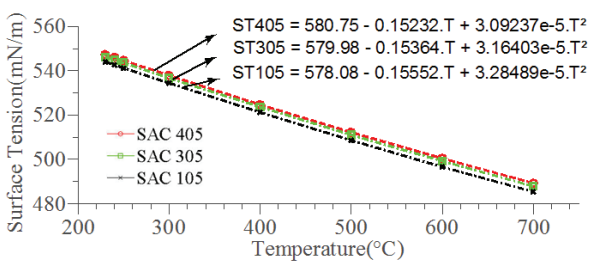

Figure 7: The surface tension of the SAC alloys depending on the temperature

Table 3: The calculated densities and surface tension of the solder alloy

Solder Type	*Average Surface Tension (mN/m^2)	Density (g/cm^3)
SAC405	546.0	7.384
SAC305	544.9	7.361
SAC105	542.6	7.316
*Average = average values taken in a range of 230°C to 250°C		

A comparison was made between the obtained result in Table 3 and the standard value from literature in [15], as well as the experimental value obtained by Huang et al. [16]. The accounted difference was 0.9% and 4.6%, respectively. The small deviation in results here may arise from the strong tendency of the elements in the alloy system to be surface active during the experiment.

4.0 CONCLUSION

In this study, DSC was used to measure three lead-free solder types with various Ag composition ratios and verify the solid-liquid-solid-phase temperatures of SAC solder. DSC is able to detect melting temperature differences caused by small composition differences in the lead-free solder. The results list the specific heat capacity, melting latent heat, solidification latent heat and phase-change temperature of the SAC solder alloys. From the study, it was found that the specific heat capacity of SAC solder increased gradually with the rise of temperature until approximately 105°C and decreasing slightly afterwards, regardless of the percentage of silver content. The results also shows that the SAC solders appear to have higher specific heat capacity values when compared to the conventional Sn-37Pb solder. The result also reveals that the specific heat capacity value is greatly dependend on the percentage value of silver content. Among the studied lead-free solders, the SAC 405 has the highest specific heat capacity value due the highest percentage of silver content (4%), and SAC 105 has the lowest C_p values, as its contain only 1% of silver. The study also presented surface tension value of various SAC solder. These results provide valuable data related to the SAC solder alloy and can be implemented as a future reference for engineer and researcher such as in developing proper numerical model [16] and to determine proper temperature conditions during reflow soldering [17-18].

ACKNOWLEDGMENTS

The authors are thankful to Universiti Teknikal Malaysia Melaka for the appreciation of the work through the awarded grant. This work was partially funded under PJP/2018/FKP(5A)9/S01585.

REFERENCES

[1] J. Bath, *Lead-free soldering*. New York: Springer, 2011.

[2] G. Henshall, "Lead-Free Alloys for BGA/CSP Components," in *Lead-Free Solder Process Development*, 2011, pp. 95–124.

[3] M.-L. Wu and J.-S. Lan, "Reliability and failure analysis of SAC 105 and SAC 1205N lead-free solder alloys during drop test events," *Microelectronics Reliability*, vol. 80, pp. 213–222, 2018.

[4] K. N. Subramaniam, *Lead-free solders: materials reliability for electronics*. Hoboken, NJ: John Wiley & Sons, 2012

[5] G. Henshall, R. Healey, R. S. Pandher, K. Sweatman, K. Howell, R. Coyle, T. Sack, P. Snugovsky, S. Tisdale, F. Hua, and H. Fu, "Addressing industry knowledge gaps regarding new Pb-free solder alloy alternatives," in 33rd IEEE/CPMT International Electronics Manufacturing Technology Conference (IEMT), Penang, 2008, pp. 1-12.

[6] B. Bader and C. Richardson, "Selected highlights from the 2017 iNEMI roadmap and projects to address identified gaps," in Pan Pacific Microelectronics Symposium (Pan Pacific), USA, 2018, pp. 1-13.

[7] B. Bottoms, M. Tsuriya, and C. Richardson, "iNEMI packaging technology roadmap highlights," in International Conference on Electronics Packaging (ICEP), Japan, 2014, pp. 188-192.

[8] A. Basak, A. Pramanik, H. Riazi, M. Silakhori, and A. Netting, "Development of Pb-Free Nanocomposite Solder Alloys," *Journal of Composites Science*, vol. 2, no. 2, pp. 1-9, 2018.

[9] S. Chellvarajoo and M. Abdullah, "Microstructure and mechanical properties of Pb-free Sn–3.0Ag–0.5Cu solder pastes added with NiO nanoparticles after reflow soldering process," *Materials & Design*, vol. 90, pp. 499-507, 2016.

[10] M. Kamarudin, A. A. Seman, and N. M. Sharif, "Effect of Aluminium and Silicon to IMC Formation in Low Ag-SAC Solder," *Materials Science Forum*, vol. 819, pp. 63–67, 2015.

[11] V. Niranjani, B. C. Rao, R. Sarkar, and S. Kamat, "The influence of addition of nanosized molybdenum and nickel particles on creep behavior of Sn–Ag lead free solder alloy," *Journal of Alloys and Compounds*, vol. 542, pp. 136–141, 2012.

[12] Q.B. Tao, L. Benabou, V.N. Le, H. Hwang, and D.B. Lu, "Viscoplastic characterization and post-rupture microanalysis of a novel lead-free solder with small additions of Bi, Sb and Ni," *Journal of Alloys and Compounds*, vol. 694, pp. 892–904, 2017.

[13] Z. Moser, W. Gasior, A. Debski, and J. Pstrus, "SURDAT - Database of physical properties of lead-free solders," *Journal of Minning and Metallurgy B: Metallurgy*, vol. 43, no. 2, pp. 125–130, 2007.

[14] Y.M. Leong and A.S.M.A. Haseeb, "Soldering characteristics and mechanical properties of Sn-1.0Ag-0.5Cu solder with minor aluminum addition," *Materials*, vol. 9, no. 7, pp. 1–17, 2016.

[15] O. Krammer, "Modelling the self-alignment of passive chip components during reflow soldering," *Microelectronics Reliability*, vol. 54, no. 2, pp. 457–463, 2014.

[16] A.M. Najib, M.Z. Abdullah, A.A. Saad, Z. Samsudin, and F. Che Ani, "Numerical simulation of self-alignment of chip resistor components for different silver content during reflow soldering," *Microelectronics Reliability*, vol. 79, pp. 69–78, 2017.

[17] A.M. Najib, M.Z. Abdullah, C.Y. Khor, and A.A. Saad, "Experimental and numerical investigation of 3D gas flow temperature field in infrared heating reflow oven with circulating fan," *International Journal of Heat and Mass Transfer*, vol. 87, pp. 49–58, 2015.

[18] A.M. Najib, M.Z. Abdullah, A.A. Saad, Z. Samsudin and F. Che Ani, "Experimental Study of Self-Alignment during Reflow Soldering Process," *Journal of Advanced Manufacturing Technology*, vol. 12, no. 1(2), pp. 355-366, 2018.